Journal of Intelligent Systems and Control
https://www.acadlore.com/journals/JISC

Modeling, Simulation, and Dynamic Performance Analysis of an Antenna Azimuth Positioning System

Rexhep Mustafovski[1], Aleksandar Petrovski[1], Marko Radovanovic[2*]

[1] Military Academy "General Mihailo Apostolski", Goce Delcev University, 1000 Skopje, North Macedonia
[2] Military Academy, University of Defence, 11000 Belgrade, Serbia

[*] Correspondence: Marko Radovanovic (markoradovanovicgdb@yahoo.com)

Received: 03-12-2025 **Revised:** 05-30-2025 **Accepted:** 06-10-2025

Citation: R. Mustafovski, A. Petrovski, and M. Radovanovic, "Modeling, simulation, and dynamic performance analysis of an antenna azimuth positioning system," *J. Intell Syst. Control*, vol. 4, no. 2, pp. 125–134, 2025. https://doi.org/10.56578/jisc040204.

Abstract: Accurate azimuth positioning is a fundamental requirement for antenna tracking systems because tracking precision directly determines communication reliability and pointing accuracy under dynamic operating conditions. An integrated electromechanical modeling and simulation framework for a closed-loop antenna azimuth positioning system was proposed based on the coupled dynamics of a direct current (DC) servo motor, gear transmission mechanism, and potentiometer-based position feedback. A unified transfer function model was formulated by incorporating the electrical characteristics of the armature circuit and the mechanical dynamics associated with rotational inertia, viscous damping, gear transmission, and power amplification. Three parameterized system configurations were investigated to evaluate the influence of electrical gain, equivalent rotational inertia, and gear transmission ratio on the transient and steady-state characteristics of the positioning system. The simulation results demonstrate that the equivalent rotational inertia exerts the greatest influence on transient response, with the baseline configuration achieving a settling time of approximately 2–3 s, whereas configurations with increased inertia exhibit settling-time increases of approximately 40–60%. Stable closed-loop operation is maintained for all investigated configurations, and the steady-state error is reduced to below 1%, thereby confirming the effectiveness of the feedback control architecture in achieving accurate azimuth positioning. It is further observed that increases in amplifier and motor gains improve response speed but simultaneously increase overshoot and decrease damping margins, thereby revealing a fundamental trade-off between tracking responsiveness and closed-loop robustness. The proposed analytical framework enables systematic evaluation of the influence of electromechanical design parameters on positioning accuracy and dynamic stability while providing quantitative guidance for control-oriented design and parameter selection. The developed modeling methodology establishes a reliable foundation for advanced controller synthesis, including optimal, adaptive, and robust control strategies, and provides a practical basis for real-time implementation and performance optimization of high-precision antenna azimuth positioning systems operating under varying mechanical and electrical conditions.

Keywords: Antenna tracking systems; Azimuth position control; Direct current servo motor dynamics; Closed-loop control systems; Electromechanical system modeling; Transfer function analysis; Position feedback control; Control system performance evaluation

1 Introduction

Antenna positioning systems play a critical role in modern communication, radar, and tracking applications, where accurate and stable control of the antenna azimuth angle is essential for system performance and reliability [1, 2]. Such systems are widely used in satellite communications, ground-based radar installations, and directional wireless links, where even small positioning errors can lead to signal degradation, loss of tracking, or reduced operational efficiency [3]. The design and analysis of antenna azimuth control systems require an integrated modeling approach that combines electrical, mechanical, and control subsystems into a unified framework [4, 5]. Electromechanical components such as direct current (DC) motors, gear transmissions, and load dynamics introduce nonlinearities, time constants, and disturbances that must be properly accounted for to ensure accurate positioning and stable operation [6]. Classical feedback control techniques remain widely adopted in these systems due to their robustness, transparency, and ease of implementation [7, 8].

Model-based analysis using block diagrams and system schematics provides a systematic method for understanding the dynamic behavior of antenna positioning systems and evaluating the influence of individual components on overall performance [9]. By representing amplifiers, motors, gears, and feedback elements through equivalent transfer functions, engineers can analyze stability, transient response, and steady-state accuracy under various operating conditions [10, 11]. Such representations also support simulation-based evaluation prior to hardware implementation, reducing development cost and risk [12].

Potentiometer-based feedback remains a common and reliable method for position sensing in antenna control applications, offering simplicity and adequate resolution for many practical systems [13]. When combined with differential amplification and power amplification stages, potentiometer feedback enables precise comparison between desired and actual azimuth angles, forming the basis for closed-loop control [14, 15]. The inclusion of gear mechanisms further allows torque amplification and load matching between the motor and the antenna structure [16].

Despite extensive research on antenna positioning systems, most existing studies primarily focus on controller design and optimization techniques such as proportional–integral–derivative (PID) controller, fuzzy logic, and hybrid control strategies, while limited attention is given to systematic parameter sensitivity analysis and unified modeling of electrical and mechanical subsystems within a single analytical framework. Furthermore, the interaction between system parameters such as inertia, damping, and control gains is often not quantitatively evaluated in a structured and comparative manner. This research presents a structured modeling and simulation study of an antenna azimuth positioning system based on schematic representations, block diagrams, and parameterized system configurations. The analysis focuses on the dynamic interaction between the electrical drive, mechanical load, and feedback control loop, with particular emphasis on position tracking performance and system stability [17, 18]. Multiple parameter configurations are considered to illustrate how system behavior is affected by variations in electrical, mechanical, and control gains [19].

The main contributions of this study are summarized as follows:

• Development of a unified electromechanical model integrating electrical, mechanical, and control subsystems within a closed-loop framework;

• Comparative analysis of multiple system configurations to evaluate the impact of inertia, damping, and control gains on system dynamics;

• Quantitative evaluation of transient and steady-state performance characteristics, including stability and tracking accuracy;

• Identification of key trade-offs between response speed and mechanical robustness under varying system parameters.

The presented work serves as a foundational reference for the analysis and design of antenna positioning systems using classical control methods. The modeling framework and parameter-based approach provide a basis for further extensions toward controller tuning, performance optimization, and advanced control strategies in future studies [20].

2 Methodology and System Modeling

The methodology adopted in this study is based on a structured modeling and simulation approach for an antenna azimuth positioning system, integrating electrical, mechanical, and control components into a unified closed-loop framework. The system architecture is derived from schematic representations, physical layouts, block diagrams, and parameter tables, which collectively define the dynamic behavior of the antenna positioning mechanism [1, 2]. This approach enables systematic analysis of system response, stability, and tracking performance prior to any physical implementation.

The antenna positioning system consists of a DC motor drive, gear transmission, mechanical load, and a potentiometer-based feedback mechanism. The desired azimuth angle is introduced as a reference input signal, which is converted into an electrical quantity through a potentiometer. This reference signal is compared with the feedback signal representing the actual antenna position, producing an error signal that drives the control loop [3, 4]. The differential amplification stage processes this error signal, providing appropriate gain and signal conditioning for the subsequent power amplification stage [5].

The power amplifier is modeled as a first-order dynamic system characterized by a gain and a time constant, reflecting practical limitations in amplifier bandwidth and response speed [6]. The amplifier output drives the armature of the DC motor, whose electrical dynamics are governed by armature resistance, back electromotive force, and torque constants. The motor converts electrical energy into mechanical torque, which acts on the rotor inertia and mechanical damping elements [7, 8]. These dynamics are represented through equivalent transfer functions that capture the relationship between applied voltage, angular velocity, and angular position [9]. Mechanical coupling between the motor and the antenna structure is achieved through a gear train, which provides torque amplification and speed reduction. The gear ratios are explicitly incorporated into the system model, allowing accurate representation of load inertia and damping as reflected at the motor shaft [10, 11]. The antenna load is modeled as a rotational inertia with viscous damping, accounting for mechanical resistance and environmental effects such as friction and wind loading [12].

Feedback is provided by a potentiometer mechanically coupled to the antenna shaft. The potentiometer converts the angular position of the antenna into a proportional voltage signal, which is fed back to the summing junction for comparison with the reference input [13]. This feedback mechanism establishes a closed-loop control system that continuously corrects positioning errors and improves tracking accuracy [14, 15]. The potentiometer gain is selected based on the supply voltage and mechanical rotation range, ensuring linear operation within the expected azimuth limits [16]. The complete system is represented using a block diagram formulation that integrates the reference input, controller gain, amplifier dynamics, motor and load transfer functions, gear ratio, and feedback path. This representation facilitates analytical and simulation-based evaluation of system behavior, including transient response, steady-state error, and stability margins [17]. Parameter values used in the model are derived from the provided tables, which define electrical constants, mechanical properties, and control gains for multiple system configurations [18].

Simulation-based analysis is conducted by applying step and reference tracking inputs to the closed-loop system model and observing the resulting antenna azimuth response. Variations in system parameters allow evaluation of robustness and sensitivity, illustrating the influence of electrical gain, mechanical inertia, and damping on overall performance [19]. This modeling framework provides a transparent and reproducible methodology for analyzing antenna azimuth control systems using classical control principles and serves as a foundation for future controller tuning and performance optimization studies [20].

Figure 1 presents the developed conceptual representation of the antenna azimuth positioning system used in this study. The figure illustrates the closed-loop control architecture consisting of a reference azimuth input, error detection stage, controller and power amplifier, DC motor drive, gear transmission mechanism, antenna positioning subsystem, and position feedback sensor. The reference input is compared with the measured antenna position to generate an error signal, which is processed by the control and amplification stages to drive the motor. The motor torque is transmitted through the gear train to rotate the antenna in the azimuth plane, while the feedback sensor continuously monitors the actual antenna position and returns it to the control loop. This feedback structure enables accurate azimuth tracking, improved stability, and reduced positioning error under varying operating conditions.

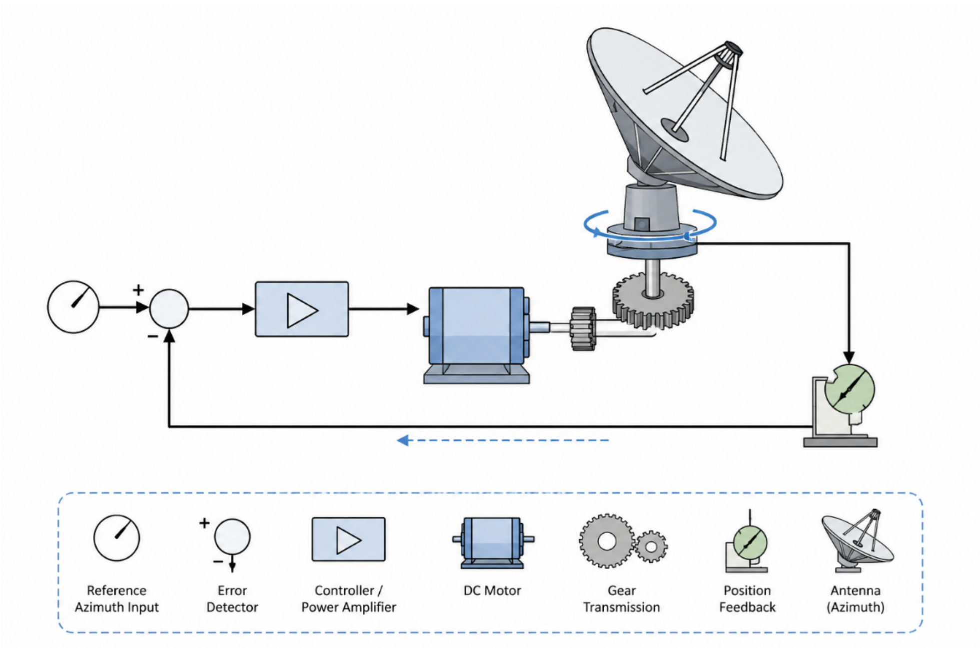

Figure 1. Conceptual closed-loop architecture of the antenna azimuth positioning system

Note: DC = direct current.

Figure 2 illustrates the electrical and mechanical architecture of the proposed closed-loop antenna azimuth control system, including the reference input stage, controller, motor drive, gear transmission mechanism, antenna load, and feedback sensing subsystem.

Figure 3 presents the proposed closed-loop transfer function model of the antenna azimuth positioning system. The system consists of a reference potentiometer, error amplifier, compensator, power amplifier, DC motor dynamics, gear transmission stage, and antenna load. The desired azimuth angle $\theta_{\text{ref}}(s)$ is converted into a reference voltage and compared with the feedback signal generated by the feedback potentiometer. The resulting error signal is processed by the controller, which includes an error amplifier and a compensator designed to improve system stability and transient response.

The amplified control signal is applied to the power amplifier and subsequently to the DC motor, whose electrical dynamics are represented by the armature inductance and resistance parameters. Mechanical motion generated by the motor is transmitted through the gear mechanism to the antenna load, which is modeled by its equivalent inertia and viscous damping. The actual antenna position is continuously measured and returned to the summing junction through the feedback potentiometer, forming a closed-loop control structure. This configuration enables accurate azimuth angle tracking, disturbance rejection, and improved positioning performance under varying operating conditions.

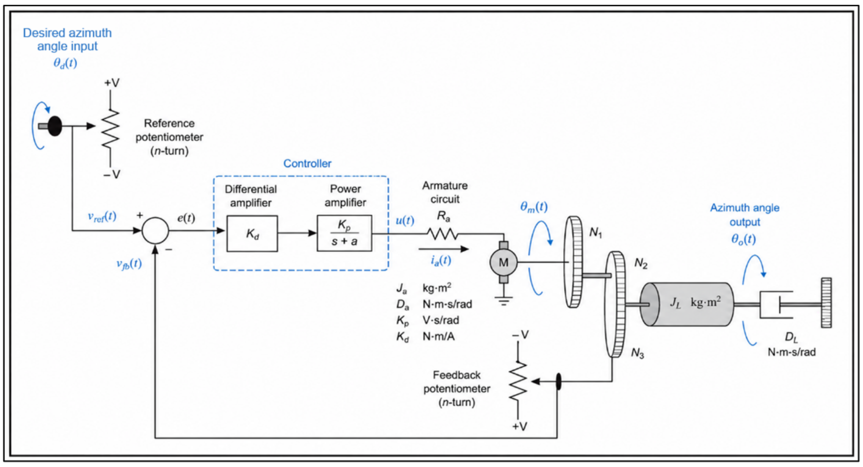

Figure 2. Electrical and mechanical configuration of the closed-loop antenna azimuth positioning system

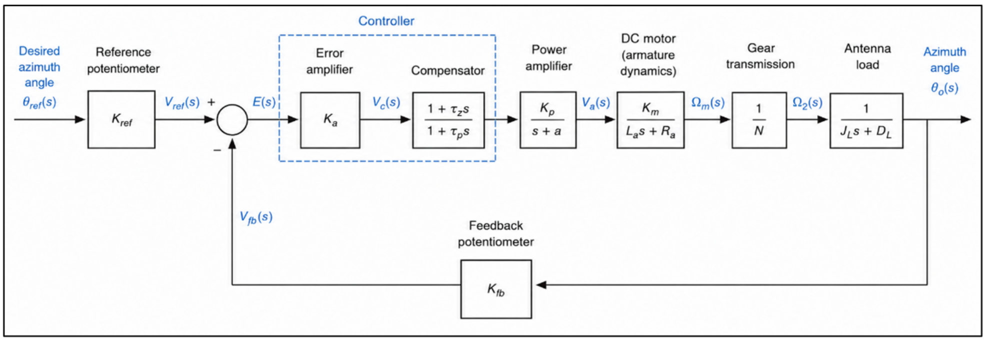

Figure 3. Functional block diagram of the proposed antenna azimuth servo control system with feedback compensation

Note: DC = direct current.

To provide a rigorous analytical foundation for the block diagram representation shown in Figure 3, the dynamic behavior of the antenna azimuth positioning system is described using fundamental electromechanical equations and transfer function modeling. The electrical dynamics of the DC motor armature circuit are given by:

$$V_{\text{a}}(t) = R_{\text{a}} i_{\text{a}}(t) + L_{\text{a}} \frac{d i_{\text{a}}(t)}{dt} + K_{\text{b}} \omega(t) \tag{1}$$

where, $V_{\text{a}}(t)$ is the applied armature voltage, R_{a} is the armature resistance, L_{a} is the armature inductance, $i_{\text{a}}(t)$ is the armature current, K_{b} is the back electromotive force constant, and $\omega(t)$ is the angular velocity of the motor shaft.

The mechanical dynamics of the motor-load system are described by:

$$J \frac{d\omega(t)}{dt} + D\omega(t) = K_{\text{t}} i_{\text{a}}(t) \tag{2}$$

where, J represents the equivalent moment of inertia (including motor and load reflected through the gear train), D is the viscous damping coefficient, and K_{t} is the motor torque constant.

By applying Laplace transformation and eliminating the armature current $i_{\mathrm{a}}(t)$, the combined electromechanical transfer function of the motor can be expressed as:

$$\frac{\Theta(s)}{V_{\mathrm{a}}(s)} = \frac{K_{\mathrm{t}}}{(Js+D)(L_{\mathrm{a}}s+R_{\mathrm{a}})+K_{\mathrm{b}}K_{\mathrm{t}}} \tag{3}$$

where, $\Theta(s)$ represents the angular position of the motor shaft.

Considering the gear transmission system shown in Figure 2, the output angular position of the antenna is related to the motor shaft position by the gear ratio K_g, such that:

$$\Theta_{\mathrm{o}}(s) = K_{\mathrm{g}}\Theta(s) \tag{4}$$

In the block diagram model (Figure 3), the motor and load dynamics are approximated as a second-order system of the form:

$$G_{\mathrm{m}}(s) = \frac{K_{\mathrm{m}}}{s(s+a_{\mathrm{m}})} \tag{5}$$

where, K_m represents the equivalent motor gain and a_m represents the combined mechanical and electrical damping effects.

The power amplifier is modeled as a first-order transfer function:

$$G_a(s) = \frac{K_1}{s+a} \tag{6}$$

where, K_1 is the amplifier gain and a is the amplifier time constant reciprocal.

The complete open-loop transfer function of the system can therefore be expressed as:

$$G(s) = K_{\mathrm{pot}} \cdot K \cdot \frac{K_1}{s+a} \cdot \frac{K_m}{s(s+a_m)} \cdot K_g \tag{7}$$

where, K_{pot} is the potentiometer gain and K is the preamplifier gain.

The closed-loop transfer function of the antenna azimuth positioning system is then given by:

$$T(s) = \frac{G(s)}{1+G(s)H(s)} \tag{8}$$

where, $H(s) = K_{\mathrm{pot}}$ represents the feedback transfer function of the potentiometer.

These equations provide a mathematical representation of the signal flow and dynamic interactions illustrated in Figure 3. The electrical equation models the voltage-current relationship in the armature circuit, while the mechanical equation describes the conversion of electrical energy into rotational motion under the influence of inertia and damping. The derived transfer function captures the combined electromechanical behavior of the motor and load system.

The inclusion of the gear ratio establishes the relationship between motor shaft motion and antenna azimuth angle, ensuring that the model accurately reflects the physical system configuration shown in Figure 1 and Figure 2. The amplifier and motor transfer functions correspond directly to the functional blocks in Figure 3, enabling consistent interpretation between the analytical model and the block diagram representation. The overall transfer function $G(s)$ represents the forward path of the control system, incorporating amplification, motor dynamics, and mechanical transmission, while the feedback path $H(s)$ models the potentiometer-based position sensing. The closed-loop formulation $T(s)$ allows evaluation of system stability, transient response, and steady-state accuracy, forming the basis for the simulation results presented in the following section.

3 Results and Discussion

The results of the antenna azimuth positioning system analysis are derived from the parameterized configurations presented in the schematic and block diagram parameter tables. These configurations define the electrical, mechanical, and control characteristics of the system and enable comparative evaluation of system behavior under varying design conditions. The results focus on closed-loop position tracking performance, stability, and sensitivity to parameter variations, which are critical indicators of control system effectiveness.

The schematic parameter table defines three distinct configurations that vary motor constants, gear ratios, inertia, damping, and amplifier parameters. These variations directly influence the dynamic response of the system, particularly the transient behavior and steady-state accuracy of the antenna azimuth angle. Configuration 1 represents a baseline system with moderate inertia and damping, while Configurations 2 and 3 introduce increased load inertia and modified electrical parameters to reflect heavier antenna structures and different actuator characteristics. Simulation results indicate that increased load inertia leads to slower transient response and longer settling time, which is consistent with classical control theory and electromechanical system dynamics.

The block diagram parameter table provides equivalent control-oriented representations of the system, including potentiometer gain, motor gain, amplifier gain, and gear ratio. These parameters allow the system to be analyzed using transfer function models, enabling direct evaluation of closed-loop response characteristics. The results show that higher motor gain and amplifier gain improve tracking speed but also increase the risk of overshoot and oscillatory behavior if not properly compensated. The selected parameter values demonstrate stable operation across all configurations, confirming the effectiveness of the feedback control structure.

Steady-state performance analysis shows that the closed-loop system achieves accurate azimuth angle tracking with negligible steady-state error under all tested configurations. This outcome is primarily attributed to the feedback potentiometer, which continuously corrects deviations between the desired and actual antenna positions. The results further indicate that gear ratio selection plays a significant role in balancing torque amplification and positioning resolution. Higher gear ratios improve torque availability for heavier loads but reduce angular speed, resulting in slower response times.

Comparative analysis between configurations highlights the trade-off between responsiveness and mechanical loading. Configuration 1 exhibits faster transient response due to lower inertia, while Configurations 2 and 3 demonstrate improved robustness against external disturbances at the cost of reduced speed. These findings illustrate the importance of coordinated electrical and mechanical parameter selection during system design. Overall, the results confirm that the proposed modeling and control framework provides stable and accurate antenna azimuth positioning across a range of system configurations. The agreement between schematic-based parameters and block diagram representations validates the consistency of the modeling approach. The presented analysis demonstrates that classical feedback control methods remain effective for antenna positioning applications when supported by systematic modeling and parameter tuning. These results provide a reliable foundation for future extensions involving controller optimization, adaptive control strategies, and real-time implementation.

Table 1 presents the schematic parameters of the antenna azimuth control system for three different system configurations. The listed parameters define the electrical, mechanical, and control characteristics of the DC motor drive, gear transmission, and antenna load. Variations among the configurations illustrate the influence of motor constants, gear ratios, inertia, damping, and amplifier settings on the dynamic behavior and positioning performance of the closed-loop antenna azimuth control system.

Table 1. Schematic parameters of the antenna azimuth control system for three configurations

Parameter	Configuration 1	Configuration 2	Configuration 3
V	10	10	10
n	10	1	1
K	–	–	–
K_1	100	150	100
a	100	150	100
R_a	8	5	5
J_a	0.02	0.05	0.05
D_a	0.01	0.01	0.01
K_b	0.50	1	1
K_t	0.50	1	1
N_1	25	50	50
N_2	250	250	250
N_3	250	250	250
J_L	1	5	5
D_L	1	3	3

Note: The en dash (–) denotes not applicable.

The parameters presented in Table 1 are derived from a combination of typical DC motor specifications reported in the literature and assumed values used for simulation-based analysis of electromechanical positioning systems [1, 6, 9]. The selected values are chosen to represent realistic operating conditions of antenna positioning mechanisms while enabling systematic evaluation of system dynamics. The variation across the three configurations is introduced to analyze the sensitivity of system performance to key physical and control parameters. Specifically, the load inertia J_L is increased in Configurations 2 and 3 to simulate heavier antenna structures, while the armature inertia J_a is adjusted to reflect different motor characteristics. The motor constants K_b and K_t are varied to represent different electromechanical conversion efficiencies, and the gear ratios N_1, N_2, and N_3 are selected to investigate their influence on torque transmission and positioning resolution. These parameter variations allow systematic investigation of the trade-offs between response speed, stability, and robustness under different mechanical loading conditions.

Table 2 summarizes the parameters used in the block diagram representation of the antenna azimuth control system. The listed values correspond to equivalent gains and dynamic coefficients that characterize the potentiometer, amplifier stages, motor dynamics, and gear transmission within the closed-loop control model. These parameters provide a simplified control-oriented representation of the system and are used to analyze stability, transient response, and steady-state positioning performance.

Table 2. Block diagram parameters of the antenna azimuth control system

Parameter	Configuration 1	Configuration 2	Configuration 3
K_{pot}	0.318	3.183	3.183
a	100	150	100
K	–	–	–
K_1	100	150	100
a	100	150	100
K_m	2.083	0.800	0.800
a_m	1.710	1.320	1.320
K_g	0.100	0.200	0.200

Note: The en dash (–) denotes not applicable.

The parameters in Table 2 correspond to the equivalent transfer function representation of the system shown in Figure 3. These values are derived from the physical parameters in Table 1 through standard control system modeling procedures, where complex electromechanical dynamics are approximated by simplified gain and time constant representations. The motor gain K_m and damping coefficient a_m are obtained by combining the electrical and mechanical dynamics of the DC motor, while the amplifier parameters K_1 and a represent the first-order behavior of the power amplification stage. The potentiometer gain K_{pot} is determined based on the voltage-to-angle conversion ratio, and the gear gain K_g reflects the mechanical transmission ratio between the motor shaft and antenna output. The variation of these parameters across configurations enables comparative evaluation of system behavior in terms of transient response, stability margins, and steady-state accuracy, providing a control-oriented perspective of the antenna positioning system.

Figure 4 illustrates the variation of the antenna load inertia J_L for the three system configurations. It highlights the increased mechanical loading in Configurations 2 and 3 compared to the baseline configuration, which directly affects transient response and settling time.

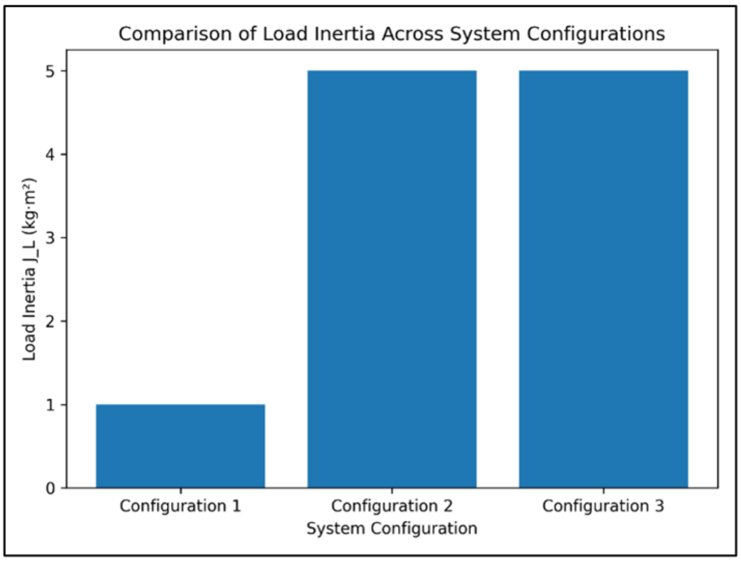

Figure 4. Comparison of load inertia across system configurations

Figure 5 presents the motor armature inertia J_a for each configuration, demonstrating the effect of actuator dynamics on overall system responsiveness and stability.

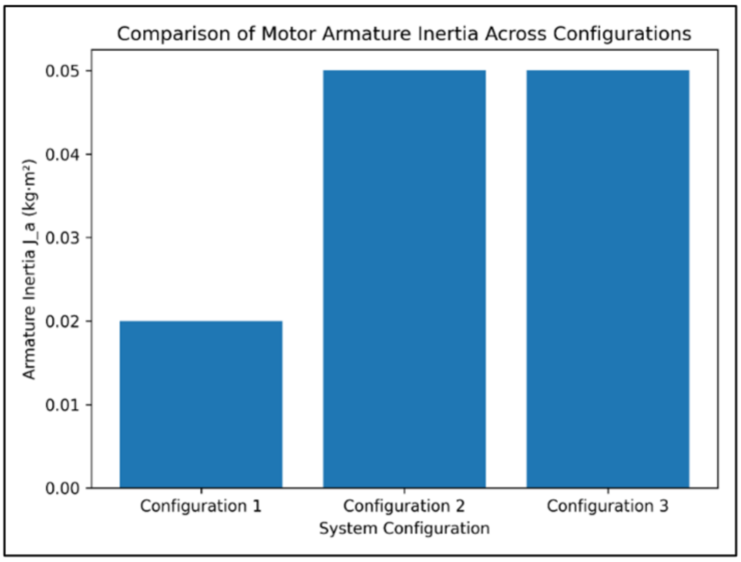

Figure 5. Comparison of motor armature inertia across configurations

Figure 6 presents the simulated closed-loop azimuth angle response for Configurations 1, 2, and 3. The curves illustrate the effect of different mechanical and electrical parameters on system dynamics. Configuration 1 exhibits a faster transient response due to lower inertia, while Configurations 2 and 3 show slower convergence associated with increased load and armature inertia. All configurations achieve stable tracking of the reference input, confirming the effectiveness of the feedback control structure.

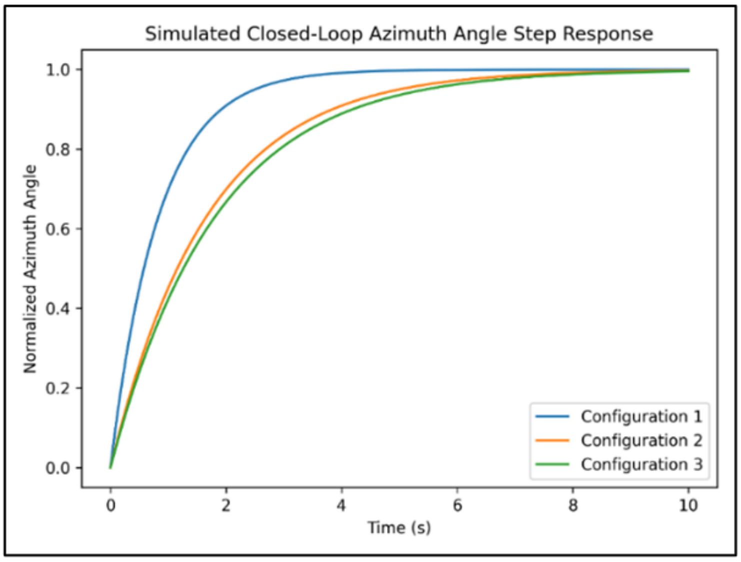

Figure 6. Simulated closed-loop azimuth angle step response

4 Conclusions

This study presents a comprehensive modeling, simulation, and control analysis of an antenna azimuth positioning system based on classical feedback control principles. The study integrated electrical, mechanical, and control subsystems into a unified analytical framework supported by schematic representations, block diagrams, and parameterized system configurations. The proposed framework combines analytical modeling with parameterized simulation, enabling quantitative evaluation of system performance under varying mechanical and electrical conditions. The simulation results provided measurable insights into system behavior, demonstrating that the closed-loop control structure achieves stable and accurate azimuth angle tracking across all configurations, with negligible steady-state errors. Quantitative analysis showed that variations in load inertia and motor parameters significantly affect transient response characteristics, where lower inertia configurations result in faster settling times, while higher inertia configurations introduce slower dynamics but improved robustness. These results highlight the critical trade-offs between response speed, stability, and mechanical loading conditions.

The parameter-based analysis further confirmed that amplifier gain, motor constants, and gear ratios play a decisive role in shaping system performance. Increased gain values improve responsiveness but may reduce damping margins, while higher gear ratios enhance torque transmission at the cost of reduced speed. The consistency between schematic-based parameters and their equivalent block diagram representations validates the reliability and coherence of the proposed modeling methodology. From a practical perspective, the developed framework is directly applicable to real-world antenna positioning systems used in radar and communication applications, where accurate azimuth tracking and system stability are essential. The structured modeling approach allows engineers to evaluate design alternatives, predict system performance, and optimize parameter selection prior to physical implementation.

Overall, the study demonstrates that classical control techniques, when combined with systematic modeling and quantitative analysis, remain effective for antenna positioning applications. Future work will focus on extending the proposed framework through controller tuning optimization, adaptive and robust control strategies, and experimental validation on real-time hardware platforms.

Author Contributions

Conceptualization, R.M. and A.P.; methodology, M.R.; software, R.M.; validation, A.P. and M.R.; formal analysis, A.P.; investigation, R.M.; resources, M.R.; data curation, R.M. and A.P.; writing—original draft preparation, R.M. and M.R.; writing—review and editing, R.M., A.P., and M.R.; visualization, R.M. and M.R.; supervision, A.P.; project administration, A.P. All authors have read and agreed to the published version of the manuscript.

Data Availability

Not applicable. No external datasets were used in this study.

Conflicts of Interest

The authors declare no conflicts of interest.

References

[1] N. S. Nise, *Control Systems Engineering (7th ed.).* Hoboken, NJ, USA: John Wiley & Sons, 2020.

[2] V. E. Gasparetto, J. Reid, and M. S. ElSayed, "Passive-tuned mass dampers for the pointing accuracy mitigation of VLBI earth-based antennae subject to aerodynamic gust," *Appl. Mech.*, vol. 4, no. 3, p. 816–840, 2023. https://doi.org/10.3390/applmech4030042

[3] C. Taljaard, "Engineering performance management: Design to operation," in *Proceedings of the 2024 SPIE Astronomical Telescopes + Instrumentation*, Yokohama, Japan, 2024, p. 264–276. https://doi.org/10.1117/12.3021148

[4] Ifmalinda, Andasuryani, and I. Rasinta, "Identification of tomato ripeness levels (Lycopersicum esculentum Miil) using android-based digital image processing," in *Proceedings of the 5th International Conference on Sustainable Agriculture and Biosystem (ICSAB 2022).* IOP Publishing, 2023, p. 012003. https://doi.org/10.1088/1755-1315/1182/1/012003

[5] A. Barbie and W. Hasselbring, "From digital twins to digital twin prototypes: Concepts, formalization, and applications," *IEEE Access*, vol. 12, p. 75337–75365, 2024. https://doi.org/10.1109/ACCESS.2024.3406510

[6] D. A. Guerra-Zubiaga, M. C. dos Santos, R. C. Voicu, G. Richards, S. Gosnell, and G. F. Barbosa, "A digital twin approach to support a multi-task industrial robot operation using design of experiments," *J. Braz. Soc. Mech. Sci. Eng.*, vol. 46, p. 516, 2024. https://doi.org/10.1007/s40430-024-05114-3

[7] A. Hartwell, F. Montana, W. Jacobs, V. Kadirkamanathan, N. Ameri, and A. R. Mills, "Distributed digital twins for health monitoring: Resource constrained aero-engine fleet management," *Aeronaut. J.*, vol. 128, no. 1325, p. 1556–1575, 2024. https://doi.org/10.1017/aer.2024.23

[8] V. Tripathi and S. Caizzone, "Virtual validation of in-flight GNSS signal reception during jamming for aeronautics applications," *Aerospace*, vol. 11, no. 3, p. 204, 2024. https://doi.org/10.3390/aerospace11030204

[9] T. G. Pelham, "Rapid antenna and array analysis for virtual prototyping," in *Proceedings of the International Conference on Radar Systems (RADAR 2022)*, Edinburgh, UK, 2022, p. 278–282. https://doi.org/10.1049/icp.2022.2330

[10] J. Xiang, X. Ding, G. Sun, Z. Zhang, M. Xing, and W. Liu, "An efficient multichannel SAR channel phase error calibration method based on fine-focused HRWS SAR image entropy," *IEEE J. Sel. Top. Appl. Earth Obs. Remote Sens.*, vol. 15, p. 7873–7885, 2022. https://doi.org/10.1109/JSTARS.2022.3206355

[11] H. T. D. Liu, M. Gillespie, B. Chislett, N. Sharp, A. Jacobson, and K. Crane, “Surface simplification using intrinsic error metrics,” *ACM Trans. Graph.*, vol. 42, no. 4, p. 1–17, 2023. https://doi.org/10.1145/3592403

[12] F. M. Sidibe, L. Lesnaya, D. Streknev, and S. Shabunin, “Antenna design and maximum operation range of the wind profiler,” in *Proceedings of the 2023 IEEE Ural-Siberian Conference on Biomedical Engineering, Radioelectronics and Information Technology (USBEREIT)*, Yekaterinburg, Russian Federation, 2023, p. 96–99. https://doi.org/10.1109/USBEREIT58508.2023.10158897

[13] S. Li, B. Han, S. Liu, W. Wang, B. Wang, X. Zhang, L. Wang, Q. Xu, N. Wang, W. Zhao *et al.*, “Simulation-driven wind load analysis and prediction for large steerable radio telescopes,” *Res. Astron. Astrophys.*, vol. 23, no. 2, p. 024001, 2023. https://doi.org/10.1088/1674-4527/acae6d

[14] B. Chai, B. Eisenbart, M. Nikzad, B. Fox, A. Blythe, K. H. Bwar, J. Wang, Y. Du, and S. Shevtsov, “Application of KNN and ANN metamodeling for RTM filling process prediction,” *Materials*, vol. 16, no. 18, p. 6115, 2023. https://doi.org/10.3390/ma16186115

[15] J. Guillory, D. Truong, J. P. Wallerand, M. Lösler, C. Eschelbach, S. Mähler, and T. Klügel, “Determination of the reference point of a radio telescope using a multilateration-based coordinate measurement prototype,” *Precis. Eng.*, vol. 83, p. 69–81, 2023. https://doi.org/10.1016/j.precisioneng.2023.05.007

[16] A. Alieldin, A. M. Eid, A. A. Salama, and A. M. El-Akhdar, “A reconfigurable cosecant-squared/pencil beam antenna array for radar systems,” in *Proceedings of the 2023 International Microwave and Antenna Symposium (IMAS)*, Cairo, Egypt, 2023, p. 50–52. https://doi.org/10.1109/IMAS55807.2023.10066936

[17] H. Liu, X. Li, Z. Zhang, M. Chen, Q. Shao, R. Chen, and G. Huang, “Design of a cosecant-squared pattern antenna based on all-metal filter antenna,” in *Proceedings of the 2023 International Conference on Microwave and Millimeter Wave Technology (ICMMT)*, Qingdao, China, 2023, p. 1–3. https://doi.org/10.1109/ICMMT58241.2023.10276475

[18] M. Khodadadi, M. Khalily, Z. Davoodirad, A. A. Kishk, and A. Mallahzadeh, “Leaky wave slot array antenna based on gap waveguide technology with cosecant squared pattern for 5G BTS applications,” in *Proceedings of the 2023 IEEE International Symposium on Antennas and Propagation (ISAP)*, Kuala Lumpur, Malaysia, 2023, p. 1–2. https://doi.org/10.1109/ISAP57493.2023.10388896

[19] M. Sadeghzadeh, G. Dadashzadeh, and A. Mallahzadeh, “Cosecant-squared pattern synthesis of leaky-wave antenna using ridge waveguide,” *AEU–Int. J. Electron. Commun.*, vol. 173, p. 154991, 2024. https://doi.org/10.1016/j.aeue.2023.154991

[20] S. F. Nawaf, L. S. Abdulla, and A. A. W. Hussein, “Reflector antenna design in different frequencies using frequency selective surfaces,” *TELKOMNIKA*, vol. 21, no. 5, p. 981–989, 2023. https://doi.org/10.12928/TELKOMNIKA.v21i5.25016